Structural Engineering and Mechanics, Vol. 8, No. 2 (1999) 151-164
DOI: http://dx.doi.org/10.12989/sem.1999.8.2.151

Nonlinear vibration of Mindlin plate subjected to moving forces including the effect of weight of the plate

Rong-Tyai Wang† and Nai-Yi Kuo‡

Department of Engineering Science, National Cheng Kung University, Tainan, Taiwan, R.O.C.

Abstract. The large deflection theory of the Mindlin plate and Galerkin's method are employed to examine the static responses of a plate produced by the weight of the plate, and the dynamic responses of the plate caused by the coupling effect of these static responses with a set of moving forces. Results obtained by the large deflection theory are compared with those by the small deflection theory. The results indicate that the effect of weight of the plate increases the modal frequencies of the structure. The deviations of dynamic transverse deflection and of dynamic bending moment produced by a moving concentrated force between the two theories are significant for a thin plate with a large area. Both dynamic transverse deflection and dynamic bending moment obtained by the Mindlin plate theory are greater than those by the classical plate.

Key words: large deflection theory; Mindlin plate; weight; moving force.

1. Introduction

Plates are extensively encountered in structures; e.g., floors, decks of a bridge and decks of a ship. By neglecting the weight of a plate, the small deflection theory is adopted to examine the vibration of the plate due to an external load. However, the weight of the plate is occasionally heavier than the magnitude of the external load acting on the plate. Therefore, neglecting the weight of the plate and taking the small deflection theory in the study of vibration of the plate may cause unrealistic responses to the structure. To correct such errors the large deflection theory for the plate should be considered. Furthermore, the weight of the plate should be accounted for while obtaining precise responses of the structure.

The classical plate model is normally adopted to study the responses of a plate caused by a static load. Neglecting the effect of transverse shear deformation of the model may underestimate the transverse deflection of the plate either as the static load is not uniformly distributed or as the plate is moderately thick. Due to this reason, the effect of shear deformation should be included for obtaining a precise deflection of the plate. Omitting the effects of rotatory inertia and shear deformation of the model leads the velocity of a bending wave in the plate to be unrealistic while a moderately thick plate is subjected to a dynamic loading within a high frequency range. To eradicate this unreasonable phenomenon, both the rotatory inertia and the shear deformation of the

† Professor
‡ Formerly, Graduate Student

plate must be considered while examining the dynamic problems of the structure. This sort of plate model is referred to as the Mindlin plate (Mindlin 1951).

The response of a plate due to moving loads is a function of both time and velocity. Based on the small deflection theory, neglecting the effect of weight of a plate causes both the maximum deflection and the maximum moment of the plate induced by a moving load to be greater than those of the plate by the load in a static situation (Wang and Lin 1996). Moreover, the dynamic responses of the plate will be unreasonable for a heavy load. To obtain more reliable responses, the large deflection theory and the effect of weight of the Mindlin plate should be simultaneously considered in examining the dynamic responses of the plate.

In this paper, a homogeneous and isotropic plate with length a, width b, thickness h, Young's modulus E, shear modulus G, Poisson's ratio μ, bending rigidity D, shear coefficient κ and mass density ρ is considered. The large deflection theory for the Mindlin plate is adopted to examine the nonlinear vibration of the plate induced by the coupling of moving loads with the weight of the plate. Two parts are available in the study. In the initial one the equations of static equilibrium of the plate due to the weight of the plate are derived. The static responses of the plate are accounted for in deriving the equations of motion of the plate in the second part. The transverse deflection is larger than the in-plane displacements for the plate. Furthermore, the inertia of the transverse motion is more important than the in-plane inertia on dominating the transverse vibration of the plate due to an external load. The in-plane inertia of the plate is, therefore, neglected in the second part.

The effects of thickness and area of the plate on the deviations of transverse deflection and of bending moment between the large deflection theory and the small deflection theory are investigated in this study. A set of four discrete forces traversing on the plate is used to simulate a vehicle moving on the plate. The effect of the weight of the plate on the dynamic responses of the structure induced by the moving forces is also investigated. Due to the coupling effect of in-plane extensions with the transverse deflection, both the equations of static equilibrium and the equations of motion of the plate cannot be solved analytically. Therefore, the sets of mode shape functions obtained from the small deflection theory for the plate is incorporated in the Galerkin's method to solve the nonlinear problems in the current study. The findings obtained from the Mindlin plate theory and from the classical plate, respectively, are discussed.

2. Displacements-stresses relation

A plate with four simply supported and immovable edges in the Cartesian coordinates is considered. The plate is subjected to a distributed force $f(x, y, t)$. The displacements in the middle surface along these axes and the bending slopes of the plate caused by the weight of the plate are denoted as u^o, v^o, w^o, α^o and β^o, respectively. Moreover, the corresponding dynamic deformations of the plate caused by the external force are betoken as u^*, v^*, w^*, α^* and β^*, respectively. The total displacements u, v and w at any point of the plate along these axes are

$$u(x,y,z,t) = u^o(x,y) + u^*(x,y,t) - z[\alpha^o(x,y) + \alpha^*(x,y,t)] \tag{1a}$$

$$v(x,y,z,t) = v^o(x,y) + v^*(x,y,t) - z[\beta^o(x,y) + \beta^*(x,y,t)] \tag{1b}$$

$$w(x,y,z,t) = w^o(x,y) + w^*(x,y,t) \tag{1c}$$

The strain-displacement relations based on the large deflection theory are

$$\varepsilon_{xx} = \varepsilon_{xx}^{o} + \varepsilon_{xx}^{*} - z(\alpha^{o} + \alpha^{*})_{,x}, \qquad \varepsilon_{yy} = \varepsilon_{yy}^{o} + \varepsilon_{yy}^{*} - z(\beta^{o} + \beta^{*})_{,y}$$
$$\gamma_{xy} = \gamma_{xy}^{o} + \gamma_{xy}^{*} - z(\alpha^{o} + \alpha^{*})_{,y} + (\beta^{o} + \beta^{*})_{,x}$$
$$\gamma_{yz} = \gamma_{yz}^{o} + \gamma_{yz}^{*}, \qquad \gamma_{zx} = \gamma_{zx}^{o} + \gamma_{zx}^{*} \tag{2}$$

where the subscript x (or y) separated by a comma denotes the differentiation with respect to x (or y). In Eq. (2) the in-plane strains ε_{xx}^{o}, ε_{yy}^{o}, γ_{xy}^{o} and the transverse shear strains γ_{yz}^{o} and γ_{zx}^{o} of the plate are induced by the weight of the plate. Further, the dynamic in-plane strains ε_{xx}^{*}, ε_{yy}^{*}, γ_{xy}^{*} and the dynamic transverse shear strains γ_{yz}^{*} and γ_{zx}^{*} of the plate are induced by the coupling effect of the weight of the plate with the external force. These static in-plane strains (Wu and Vinson 1969) and dynamic in-plane strains are

$$\varepsilon_{xx}^{o} = u^{o}{}_{,x} + 0.5(w^{o}{}_{,x})^2, \quad \varepsilon_{yy}^{o} = v^{o}{}_{,y} + 0.5(w^{o}{}_{,y})^2,$$
$$\gamma_{xy}^{o} = u^{o}{}_{,y} + v^{o}{}_{,x} + w^{o}{}_{,x}\, w^{o}{}_{,y}, \quad \gamma_{yz}^{o} = w^{o}{}_{,y} - \beta^{o}, \quad \gamma_{zx}^{o} = w^{o}{}_{,x} - \alpha^{o} \tag{3}$$
$$\varepsilon_{xx}^{*} = u^{*}{}_{,x} + w^{o}{}_{,x} w^{*}{}_{,x} + 0.5(w^{*}{}_{,x})^2, \quad \varepsilon_{yy}^{*} = v^{*}{}_{,y} + w^{o}{}_{,y} w^{*}{}_{,y} + 0.5(w^{*}{}_{,y})^2,$$
$$\gamma_{xy}^{*} = u^{*}{}_{,y} + v^{*}{}_{,x} + w^{o}{}_{,x} w^{*}{}_{,y} + w^{o}{}_{,y} w^{*}{}_{,x} + w^{*}{}_{,x} w^{*}{}_{,y},$$
$$\gamma_{yz}^{*} = w^{*}{}_{,y} - \beta^{*}, \quad \gamma_{zx}^{*} = w^{*}{}_{,x} - \alpha^{*} \tag{4}$$

The in-plane stress resultants n_x, n_y, n_{xy}, the transverse shear stress resultants q_x, q_y and the stress-couple resultants m_x, m_y, m_{xy} per unit length of the plate are

$$n_x = n_x^{o} + n_x^{*}, \quad n_y = n_y^{o} + n_y^{*}, \quad n_{xy} = n_{xy}^{o} + n_{xy}^{*}, \quad q_y = q_y^{o} + q_y^{*},$$
$$q_x = q_x^{o} + q_x^{*}, \quad m_x = m_x^{o} + m_x^{*}, \quad m_y = m_y^{o} + m_y^{*}, \quad m_{xy} = m_{xy}^{o} + m_{xy}^{*} \tag{5}$$

in which the quantities with the superscript o denote the quantities induced by the weight of the plate only. Moreover, the quantities with the superscript $*$ indicate the dynamic quantities induced by the coupling effect of the weight of the plate with the external force. These quantities are

$$n_x^{\upsilon} = \frac{Eh}{1-\mu^2}(\varepsilon_{xx}^{\upsilon} + \mu\varepsilon_{yy}^{\upsilon}), \quad n_y^{\upsilon} = \frac{Eh}{1-\mu^2}(\mu\varepsilon_{xx}^{\upsilon} + \varepsilon_{yy}^{\upsilon}), \quad n_{xy}^{\upsilon} = Gh\,\gamma_{xy}^{\upsilon},$$
$$q_y^{\upsilon} = \kappa Gh\,\gamma_{yz}^{\upsilon}, \quad q_x^{o} = \kappa Gh\,\gamma_{zx}^{o}, \quad m_x^{\upsilon} = -D(\alpha^{\upsilon}{}_{,x} + \mu\beta^{\upsilon}{}_{,y}),$$
$$m_y^{\upsilon} = -D(\mu\alpha^{\upsilon}{}_{,x} + \beta^{\upsilon}{}_{,y}), \quad m_{xy}^{\upsilon} = -0.5(1-\mu)D(\alpha^{\upsilon}{}_{,y} + \beta^{\upsilon}{}_{,x}) \tag{6}$$

where the superscript υ denotes o or $*$.

3. Static equilibrium

The equations of equilibrium of the plate obtained from the principle of virtual work are

$$n_x^{o}{}_{,x} + n_{xy}^{o}{}_{,y} = 0, \quad n_{xy}^{o}{}_{,x} + n_y^{o}{}_{,y} = 0 \tag{7a, b}$$
$$D[\alpha^{o}{}_{,xx} + 0.5(1-\mu)\alpha^{o}{}_{,yy} + 0.5(1+\mu)\beta^{o}{}_{,xy}] + \kappa Gh(w^{o}{}_{,x} - \alpha^{o}) = 0 \tag{7c}$$
$$D[0.5(1+\mu)\alpha^{o}{}_{,xy} + 0.5(1-\mu)\beta^{o}{}_{,xx} + \beta^{o}{}_{,yy}] + \kappa Gh(w^{o}{}_{,y} - \beta^{o}) = 0 \tag{7d}$$
$$(n_x^{o} w^{o}{}_{,x})_{,x} + (n_y^{o} w^{o}{}_{,y})_{,y} + n_{xy}^{o} w^{o}{}_{,x})_{,y} + (n_{xy}^{o} w^{o}{}_{,y})_{,x}$$

$$+\kappa Gh(w^o{}_{,x}-\alpha^o)_{,x}+\kappa Gh(w^o{}_{,y}-\beta^o)_{,y}+\rho gh=0 \tag{7e}$$

in which g denotes the constant of gravity.

By introducing the stress function ϕ^o such that

$$n_x^o=\phi^o{}_{,yy},\quad n_y^o=\phi^o{}_{,xx},\quad n_{xy}^o=-\phi^o{}_{,xy} \tag{8}$$

Eq. (7e) can be rewritten as this form

$$L(\phi^o, w^o)+\kappa Gh(w^o{}_{,x}-\alpha^o)_{,x}+\kappa Gh(w^o{}_{,y}-\beta^o)_{,y}+\rho gh=0 \tag{9}$$

in which the operator L is

$$L(A,B)=A_{,xx}B_{,yy}+A_{,yy}B_{,xx}-2A_{,xy}B_{,xy}$$

Eliminating α^o and β^o from Eq. (9) by using Eqs. (7c) and (7d) yields that the governing equation of transverse deflection w^o of the plate is

$$\Delta\Delta w^o=\frac{\rho gh}{D}+\left(\frac{1}{D}-\frac{\Delta}{\kappa Gh}\right)L(\phi^o, w^o) \tag{10}$$

in which Δ is the harmonic operator. The compatibility condition can be expressed as the form (Fung 1965)

$$\Delta\Delta\phi^o+0.5EhL(w^o, w^o)=0 \tag{11}$$

4. Equations of motion

By neglecting the in-plane inertia, the equations of motion of the plate can be obtained from the Hamilton's principle as these forms

$$n_x^*{}_{,x}+n_{xy}^*{}_{,y}=0,\quad n_{xy}^*{}_{,x}+n_y^*{}_{,y}=0 \tag{12a, b}$$

$$n_x^o w^*{}_{,xx}+n_y^o w^*{}_{,yy}+2n_{xy}^o w^*{}_{,xy}+n_x^*(w^o+w^*)_{,xx}+n_y^*(w^o+w^*)_{,yy}$$
$$+2n_{xy}^*(w^o+w^*)_{,xy}+q_{x,x}^*+q_{y,y}^*+f(x,y,t)=\rho h w^*{}_{,tt} \tag{12c}$$

$$-m_x^*{}_{,x}-m_{xy}^*{}_{,y}+q_x^*=\rho I\alpha^*{}_{,tt},\quad -m_{xy}^*{}_{,x}-m_y^*{}_{,y}+q_y^*=\rho I\beta^*{}_{,tt} \tag{12d, e}$$

Introducing the dynamic stress function ϕ^* such that

$$(n_x^*, n_y^*, n_{xy}^*)=(\phi^*{}_{,yy}, \phi^*{}_{,xx}, -\phi^*{}_{,xy}) \tag{13}$$

and employing Eqs. (13) and (8) into Eq. (12c) yields

$$L(\phi^o, w^*)+L(\phi^*, w^o+w^*)+q_x^*{}_{,x}+q_y^*{}_{,y}+f(x,y,t)=\rho h w^*{}_{,tt} \tag{14}$$

Eqs. (12d), (12e) and (14) constitute the equations of motion of the plate. The compatibility condition of the plate can be expressed as (Celep 1980)

$$\Delta\Delta\phi^*+EhL(w^o, w^*)+0.5EhL(w^*, w^*)=0 \tag{15}$$

5. Non-dimensional forms

By introducing the following non-dimensional variables

$$(\bar{w}^{\,o}, \bar{w}^{\,*}) = (w^o, w^*)/h, \quad \bar{x} = x/a, \quad \bar{y} = y/b, \quad \lambda = a/b, \quad r = h/a, \quad \bar{g} = \rho g a^4/D,$$
$$(\bar{\phi}^{\,o}, \bar{\phi}^{\,*}) = (\phi^o, \phi^*)/Eh^3, \quad \varepsilon = \kappa G h a^2/D, \quad \bar{\Delta} = a^2\Delta, \quad \bar{L} = a^2 b^2 L, \quad \bar{t} = t(D/\rho h a^4)^{1/2},$$
$$\eta = \kappa G h a^2/D, \quad \bar{\alpha}^{\,*} = a\alpha^*/h, \quad \bar{\beta}^{\,*} = b\beta^*/h, \quad \bar{f} = fa^4/Dh, \quad \bar{m}_{\bar{x}}^{\,*} = a^2 m_x^*/Dh,$$
$$\bar{m}_{\bar{y}}^{\,*} = b^2 m_y^*/Dh, \quad \bar{m}_{\bar{x}\bar{y}}^{\,*} = abm_{xy}^*/Dh, \quad \bar{q}_{\bar{x}}^{\,*} = aq_x^*/\kappa G h^2, \quad \bar{q}_{\bar{y}}^{\,*} = bq_y^*/\kappa G h^2$$

Eqs. (10) and (11) are expressed as the non-dimensional forms respectively.

$$\bar{\Delta}\bar{\Delta}\bar{w}^{\,o} = \bar{g} + 12(1-\mu^2)\lambda^2(1-\bar{\Delta}/\varepsilon)\bar{L}(\bar{\phi}^{\,o}, \bar{w}^{\,o}) \tag{16}$$
$$\bar{\Delta}\bar{\Delta}\bar{\phi}^{\,o} + 0.5\lambda^2\bar{L}(\bar{w}^{\,o}, \bar{w}^{\,o}) = 0 \tag{17}$$

Moreover, the non-dimensional forms of Eqs. (12d), (12e), (14) and (15) are

$$\frac{\partial \bar{m}_{\bar{x}}^{\,*}}{\partial \bar{x}} + \lambda^2 \frac{\partial \bar{m}_{\bar{x}\bar{y}}^{\,*}}{\partial \bar{y}} - \eta \bar{q}_{\bar{x}}^{\,*} + \frac{r^2}{12}\frac{\partial^2 \bar{\alpha}^*}{\partial \bar{t}^2} = 0 \tag{18a}$$

$$\frac{\partial \bar{m}_{\bar{x}\bar{y}}^{\,*}}{\partial \bar{x}} + \lambda^2 \frac{\partial \bar{m}_{\bar{y}}^{\,*}}{\partial \bar{y}} - \eta \bar{q}_{\bar{y}}^{\,*} + \frac{r^2}{12}\frac{\partial^2 \bar{\beta}^*}{\partial \bar{t}^2} = 0 \tag{18b}$$

$$-12(1-\mu^2)\lambda^2[\bar{L}(\bar{\phi}^o, \bar{w}^*) + \bar{L}(\bar{\phi}^*, \bar{w}^o + \bar{w}^*)] - \eta\left(\frac{\partial \bar{q}_{\bar{x}}^{\,*}}{\partial \bar{x}} + \lambda^2 \frac{\partial \bar{q}_{\bar{y}}^{\,*}}{\partial \bar{y}}\right)$$
$$+ \frac{\partial^2 \bar{w}^*}{\partial \bar{t}^2} = \bar{f}(\bar{x}, \bar{y}, \bar{t}) \tag{18c}$$

$$\bar{\Delta}\bar{\Delta}\bar{\phi}^{\,*} + \lambda^2\bar{L}(\bar{w}^o, \bar{w}^*) + 0.5\lambda^2\bar{L}(\bar{w}^*, \bar{w}^*) = 0 \tag{19}$$

The boundary conditions of the plate are

a. along $\bar{x}$ =0 or $\bar{x}$ =1,

$$\bar{u}^{\upsilon} = \bar{v}^{\upsilon} = \bar{w}^{\upsilon} = \bar{\beta}^{\upsilon} = \bar{m}_{\bar{x}}^{\,\upsilon} = 0 \tag{20a}$$

b. along $\bar{y}$ =0 or $\bar{y}$ =1,

$$\bar{u}^{\upsilon} = \bar{v}^{\upsilon} = \bar{w}^{\upsilon} = \bar{\alpha}^{\upsilon} = \bar{m}_{\bar{y}}^{\,\upsilon} = 0 \tag{20b}$$

where the superscript υ denotes o or $*$.

6. Static responses

The analytic solutions of the coupling nonlinear differential Eqs. (16) and (17) cannot be found. Therefore, the Galerkin's method is adopted to solve these coupling equations. The transverse deflection $\bar{w}^o$ of the plate is supposed to be the form

$$\bar{w}^{\,o} = \sum_{i=1}\sum_{j=1} A_{ij}^o \sin(i\pi\bar{x})\sin(j\pi\bar{y}) \tag{21}$$

Substituting $\bar{w}^o$ into Eq. (17) and solving $\bar{\phi}^o$, then substituting $\bar{w}^o$ and $\bar{\phi}^o$ into Eq. (16), multiplying by $\sin(p\pi\bar{x})\sin(r\pi\bar{y})$ and double integrating the result from $\bar{x}$=0 to $\bar{x}$=1 and from $\bar{y}$ =0 to $\bar{y}$=1 yield a system of nonlinear equations, which can be expressed symbolically as the form

$$\pi^4(p^2+\lambda^2 r^2)^2 A_{pr}^o = \frac{4\bar{g}}{pr\pi^2}[1-(-1)^p][1-(-1)^r]+N_{pr}^o \tag{22}$$

in which N_{pr}^o is

$$N_{pr}^o = 48(1-\mu^2)\lambda^2\int_0^1\int_0^1(1-\bar{\Delta}/\varepsilon)\bar{L}(\bar{\phi}^o,\bar{w}^o)\sin(p\pi\bar{x})\sin(r\pi\bar{y})\,d\bar{x}\,d\bar{y}$$

Eq. (22) can be only solved by numerical methods. To solve Eq. (22) initial approximations of the solution are required. The constants A_{ij}^o obtained from the small deflection theory of the plate due to the weight of the plate can be taken as initial approximations. These constants A_{pr}^o of Eq. (22) can then be calculated by employing Broyden's method (1965) with these initial approximations.

7. Forced vibration

Based on the small deflection theory, any two distinct sets of mode shape functions of the plate have been shown to be orthogonal (Wang and Lin 1996). Therefore, these sets of mode shape functions are employed in the Galerkin's method for examining the forced vibration of the plate in this section. Expressing the dynamic responses of the plate into the following forms

$$[\bar{w}^*(\bar{x},\bar{y},\bar{t}),\ \bar{\alpha}^*(\bar{x},\bar{y},\bar{t}),\ \bar{\beta}^*(\bar{x},\bar{y},\bar{t})] = \sum_{i=1}\sum_{j=1}A_{ij}^*(\bar{t})[W^{(ij)}(\bar{x},\bar{y}),\ \Psi_{\bar{x}}^{(ij)}(\bar{x},\bar{y}),\ \Psi_{\bar{y}}^{(ij)}(\bar{x},\bar{y})] \tag{23a}$$

$$[\bar{q}_{\bar{x}}^*(\bar{x},\bar{y},\bar{t}),\ \bar{q}_{\bar{y}}^*(\bar{x},\bar{y},\bar{t})] = \sum_{i=1}\sum_{j=1}A_{ij}^*(\bar{t})[Q_{\bar{x}}^{(ij)}(\bar{x},\bar{y}),\ Q_{\bar{y}}^{(ij)}(\bar{x},\bar{y})] \tag{23b}$$

$$[\bar{m}_{\bar{x}}^*(\bar{x},\bar{y},\bar{t}),\ \bar{m}_{\bar{y}}^*(\bar{x},\bar{y},\bar{t}),\ \bar{m}_{\bar{x}\bar{y}}^*(\bar{x},\bar{y},\bar{t})] = \sum_{i=1}\sum_{j=1}A_{ij}^*(\bar{t})[M_{\bar{x}}^{(ij)}(\bar{x},\bar{y}),\ M_{\bar{y}}^{(ij)}(\bar{x},\bar{y}),\ M_{\bar{x}\bar{y}}^{(ij)}(\bar{x},\bar{y})] \tag{23c}$$

where $A_{ij}^*(\bar{t})$ is the ijth modal amplitude and the corresponding set of mode shape functions are listed in Appendix A.

Substituting Eqs. (23a)~(23c) into Eqs. (18a)~(18c) yields

$$\sum_{i=1}\sum_{j=1}A_{ij}^*\left(\frac{\partial M_{\bar{x}}^{(ij)}}{\partial\bar{x}}+\lambda^2\frac{\partial M_{\bar{x}\bar{y}}^{(ij)}}{\partial\bar{y}}-\eta Q_{\bar{x}}^{(ij)}\right)+\frac{r^2}{12}\sum_{i=1}\sum_{j=1}\Psi_{\bar{x}}^{(ij)}\frac{d^2A_{ij}^*}{d\bar{t}^2}=0, \tag{24a}$$

$$\sum_{i=1}\sum_{j=1}A_{ij}^*\left(\frac{\partial M_{\bar{x}\bar{y}}^{(ij)}}{\partial\bar{x}}+\lambda^2\frac{\partial M_{\bar{y}}^{(ij)}}{\partial\bar{y}}-\eta Q_{\bar{y}}^{(ij)}\right)+\frac{r^2}{12}\sum_{i=1}\sum_{j=1}\Psi_{\bar{y}}^{(ij)}\frac{d^2A_{ij}^*}{d\bar{t}^2}=0, \tag{24b}$$

$$-\eta\sum\sum A_{ij}^{*}\left(\frac{\partial Q_{\bar{x}}^{(ij)}}{\partial \bar{x}}+\lambda^2\frac{\partial Q_{\bar{y}}^{(ij)}}{\partial \bar{y}}\right)+\sum\sum W^{(ij)}\frac{d^2A_{ij}^{*}}{d\,\bar{t}^{\,2}}=$$
$$\bar{f}\ (\bar{x}\ ,\ \bar{y}\ ,\ \bar{t}\ )+12(1-\mu^2)\,\lambda^2[\bar{L}\ (\bar{\phi}^{o},\ \bar{w}^{*})+\bar{L}\ (\bar{\phi}^{*},\ \bar{w}^{o}+\bar{w}^{*})] \tag{24c}$$

Multiplying Eq. (24a) by $\Psi_{\bar{x}}^{(kl)}$, Eq. (24b) by $\Psi_{\bar{y}}^{(kl)}$, Eq. (24c) by $W^{(kl)}$ and double integrating their sum from $\bar{x}$ =0 to $\bar{x}$ =1 and from $\bar{y}$ =0 to $\bar{y}$ =1 yields

$$\frac{d^2A_{kl}^{*}}{d\bar{t}^{\,2}}+\bar{\omega}_{kl}^{2}A_{kl}^{*}-N_{kl}^{*}=\bar{f}_{kl}(\bar{t}) \tag{25}$$

in which $\bar{\omega}_{kl}$ denotes the *kl*-th modal frequency. The corresponding modal excitation $\bar{f}_{kl}$ is

$$\bar{f}_{kl}(\bar{t})=\int_0^1\int_0^1\bar{f}(\bar{x}\ ,\bar{y}\ ,\bar{t}\ )\,W^{(kl)}(\bar{x}\ ,\bar{y}\ )\,d\,\bar{x}\,d\,\bar{y}\,/s_{kl} \tag{26a}$$

where the *kl*-th modal mass s_{kl} is

$$s_{kl}=\int_0^1\int_0^1[W^{(kl)2}+\frac{r^2}{12}(\Psi_{\bar{x}}^{(kl)})^2+\frac{r^2\lambda^2}{12}(\Psi_{\bar{y}}^{(kl)})^2]\,d\,\bar{x}\,d\,\bar{y} \tag{26b}$$

In Eq. (25), the nonlinear term N_{kl}^{*} due to the coupling of the longitudinal force with the transverse deflection is

$$N_{kl}^{*}=12(1-\mu^2)\,\lambda^2\int_0^1\int_0^1 W^{(kl)}[\bar{L}\,(\bar{\phi}^{o},\bar{w}^{*})+\bar{L}\,(\bar{\phi}^{*},\bar{w}^{o}+\bar{w}^{*})]\,d\,\bar{x}\,d\,\bar{y}\ /s_{kl} \tag{27}$$

in which $\bar{\phi}^{*}$ is solved from Eq. (19).

Eq. (25) constitutes a system of nonlinear differential equations. The analytic solutions of Eq. (25) cannot be obtained. Therefore, the Runge-Kutta method is adopted in the numerical computation to search the solutions. Herein, the initial conditions of these dynamic responses are

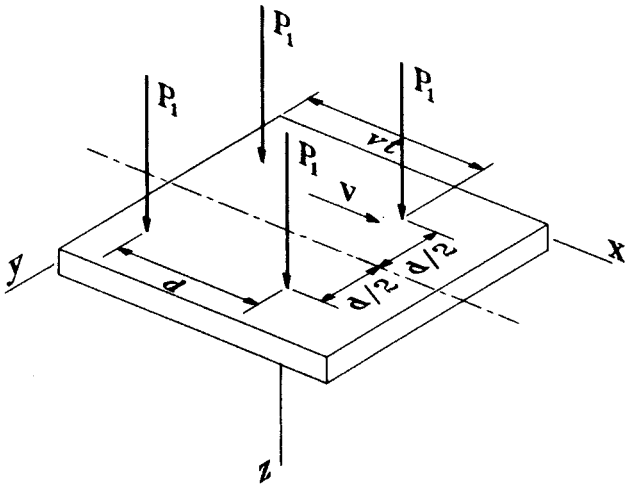

Fig. 1 A set of four discrete forces traversing on the plate

set at zeros.

To examine the dynamic responses of the plate induced by a moving force, a set of four discrete forces traversing on the plate at a constant velocity v is depicted in Fig. 1. The magnitude of each force is P_1. The form of this set of forces is

$$f(x,y,t)=P_1[\delta(x-vt)+\delta(x-vt+d)]\cdot[\delta(y-0.5b-0.5d)+\delta(y-0.5b+0.5d)] \quad (28)$$

where d is the distance between two forces and δ is the impulse function.

8. Examples

In this section, a square aluminum plate (λ=1) is taken as an example. The material constants of aluminum are μ=0.3, κ=0.85, E=70Gpa and ρ=2710 kg/m^3. Furthermore, the terms of i=1~8 and j =1~8 are considered in the numerical computations.

8.1. Static results

According to the small deflection theory for plates, the static in-plane deformations of a plate are not related to the static transverse deflection of the plate. Based on the theory, the static transverse deflection of the Mindlin plate induced by the weight of the plate is, therefore, the same as that of the classical plate. According to the large deflection theory for plates, the effect of transverse shear deformation causes the static transverse deflection of the Mindlin plate to be greater than that of the classical plate. However, the effect of transverse shear deformation is negligible as the ratio of thickness to either length or width of the plate is small. Owing to this reason, the static transverse deflections obtained by the large deflection theory for these two plate models, respectively, are nearly the same as the ratio of thickness to either length or width and is therefore very small. The large deflection theory for plates indicates that the products of the forces of the static in-plane extensions with the static transverse deflection raise the bending stiffness of the plate. Consequently, w^o and m_x^0 of the plate predicated by the large deflection theory are

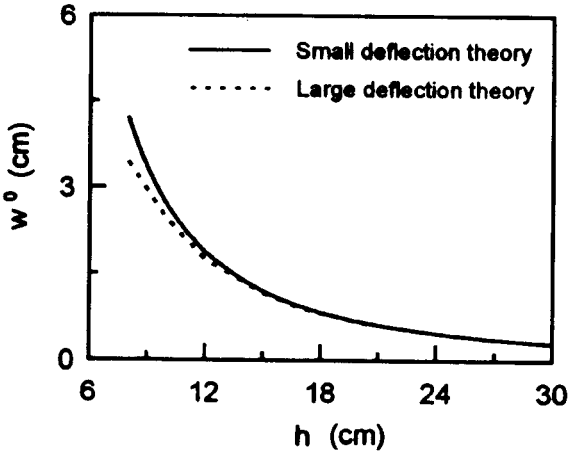

Fig. 2 The effect of thickness on w^o at the central point of a square plate (a=b=20 m)

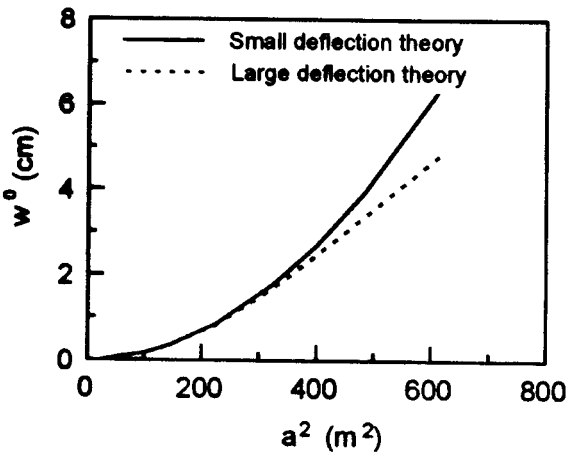

Fig. 3 The effect of area on w^o at the central point of a square plate (a=b, h=10 cm)

smaller than those predicated by the small deflection theory.

A comparison of the effects of the two deflection theories on the $w^o - h$ distribution at the central point of the plate (a=b=20m) is displayed in Fig. 2. The weight of the plate is linearly proportional to the thickness of the plate. According to the small deflection theory for plates, w^o of the plate is inversely proportional to the bending rigidity, which is proportional to a cubic order of the thickness of the plate. Based on the small deflection theory for plates, w^o of the plate is, therefore, inversely proportional to the second order of thickness of the plate. The large deflection theory for plates indicates that the forces of in-plane extensions of the plate are proportional to the second order of transverse deflection of the plate. Therefore, both the transverse deflection and the forces of in-plane extensions of a thin plate are large. Owing to this reason, results of Fig. 2 show that the deviation of w^o between the large deflection theory and the small deflection theory increases as the thickness decreases.

According to the small deflection theory for plates, w^o at the central point of the plate is the second order proportional to the area of the plate. Therefore, the bending stiffness owing to the products of forces of the in-plane extensions with w^o rises as the area of the plate increases. Consequently, results of Fig. 3 show that the deviation of w^o between the small deflection theory and the large deflection theory rises as the area of the plate increases.

8.2. Dynamic results

To investigate the effects of a set of four discrete moving forces on the dynamic responses of the plate, $4P_1$=20kN is considered. Moreover, for the convenience of discussion, the following nomenclature is introduced: small deflection theory, SDT; large deflection theory without including the effect of weight of the plate, LDTN; large deflection theory including the effect of weight of the plate, LDTW, the maximum w^* of the plate during the forces traversing on the pate, w^*_{max}; the maximum m^*_x of the plate during the forces traversing on the plate, $m^*_{x,max}$.

A comparison of three estimated histories of w^* at the central point of the Mindlin plate (a=b= 20 m, h=0.1 m) subjected to a moving concentrated force (v=30 km/hr) by SDT, LDTN and

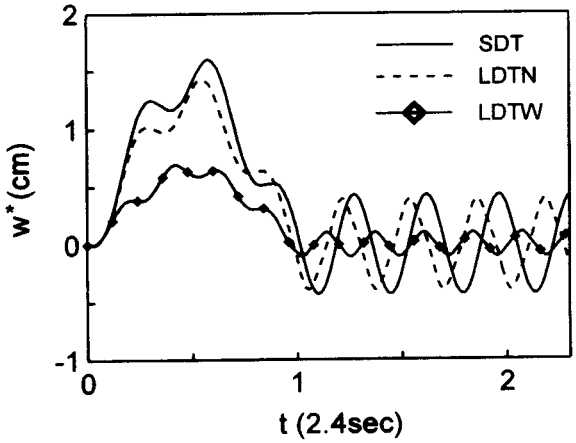

Fig. 4 Comparison of the effects of three deflection theories on the history of w^* at the central point of the Mindlin plate (a=b=20 m, h=0.1 m) due to a moving concentrated force ($4P_1$=20 kN, v=30 km/hr)

Table 1 Comparison of both effects of two different velocities and three different deflection theories on the fundamental period of the plate (a=b=20 m, h=0.1 m) due to a moving concentrated force ($4P_1$=20 kN)

	v=30 km/hr	v=90 km/hr
SDT	0.816 sec	0.816 sec
LDTN	0.768 sec	0.752 sec
LDTW	0.576 sec	0.544 sec

Table 2 Comparison of the effects of two different magnitudes of a moving concentrated force on the fundamental period of the plate (a=b= 20 m, h=0.1 m)

	$4P_1$=10 kN	$4P_1$=20 kN
SDT	0.816 sec	0.816 sec
LDTN	0.800 sec	0.752 sec
LDTW	0.568 sec	0.544 sec

LDTW, respectively, is displayed in Fig. 4. The coupling effect of the forces n_x^o, n_y^o and n_{xy}^o with w^* as well as that of n_x^*, n_y^* and n_{xy}^* with w^o stiffen the plate. Therefore, LDTW leads to the minimum w^* among these theories. The period of response w^* of the plate in the free vibration after the force has left the structure is called the fundamental period T of the plate. Based on the small deflection theory, each modal response of the plate is independent. Moreover, the first mode dominates the vibration of the plate. Therefore, the fundamental period of the plate in terms of the small deflection theory is independent on the effects of velocity and magnitude of the moving force. The fundamental period for either LDTN or LDTW depends on the coupling effect of static responses with all modal responses. A rapid moving force excites a larger number of modes of the plate than does a slow moving force. The coupling between high frequency modes and low frequency modes causes the magnitude of the fundamental period of the plate to be small for a rapid moving force, as indicated in Table 1. A moving force with a large magnitude causes a strong coupling of low frequency modes with high frequency modes of the plate. Consequently, a larger moving force causes the plate to exhibit a smaller value of the fundamental period, as indicated in Table 2. This similar phenomenon has also been observed by Chu and Herrmann (1956). The fundamental period of an initially imperfect plate is less than that of a flat plate (Celep 1980). The static deflection of the plate induced by the weight of the plate can be similarly regarded as an initial imperfection of the plate. Therefore, results in these two tables show that LDTW leads the plate to have a minimum T in the current study.

The comparisons of the three different d effects of the force on the $w^*_{max} - v$ distribution and the $m^*_{x,max} - v$ distribution of the Mindlin plate (a=b=20 m, h=0.1 m) based on LDTW are displayed in Figs. 5(a) and 5(b), respectively, to indicate that the moving concentrated force induces both the maximum dynamic deflection and the maximum dynamic bending moment of the plate among these types of forces. Therefore, the responses of the plate induced by the moving concentrated force are merely considered in the following discussions.

The comparisons of the effects of three different theories on the $w^*_{max} - v$ distribution and the

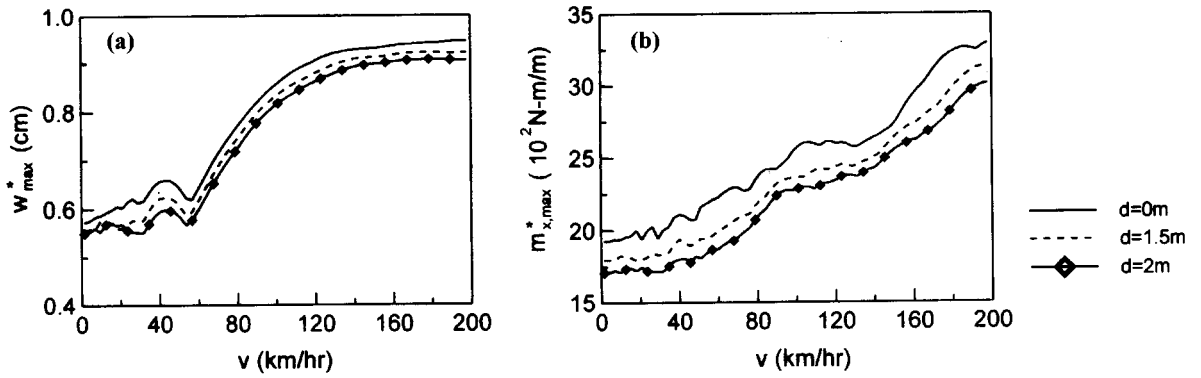

Fig. 5 Comparisons of the effects of three values d of the moving force ($4P_1$=20 kN) on: (a) $w^*_{max}-v$ and (b) $m^*_{x,max}-v$ distributions of the Mindlin plate (a=b=20 m, h=0.1 m) based on LDTW

$m^*_{x,max}-v$ distribution of the Mindlin plate (a=b=20 m, h=0.1 m) induced by a moving concentrated force are displayed in Figs. 6(a) and 6(b), respectively, to show that LDTW leads to both the minimum w^*_{max} and the minimum $m^*_{x,max}$ of the plate among these theories. These findings indicate that the weight of the plate plays a significant role on dominating the vibration of the plate.

A comparison of the two different effects of thickness on the $w^*_{max}-v$ distribution of the Mindlin plate (a=b=20 m) induced by a moving concentrated force is displayed in Fig. 7. Results of the figure shows that (a) w^*_{max} obtained by LDTW is smaller than that by LDTN, (b) w^*_{max} is larger for a thinner plate and (c) the deviation of w^*_{max} between LTDW and LTDN is larger for a thinner plate.

A comparison of the two different effects of area on the $w^*_{max}-v$ distribution of the Mindlin plate (h=0.1 m) induced by a moving concentrated force is displayed in Fig. 8. Results of the figure shows that (a) w^*_{max} obtained by LDTW is smaller than that by LDTN, (b) w^*_{max} is larger for a larger plate and (c) the deviation of w^*_{max} between LTDW and LTDN is larger for a larger plate.

The comparisons of both effects of two different theories (LDTN, LDTW) and two different

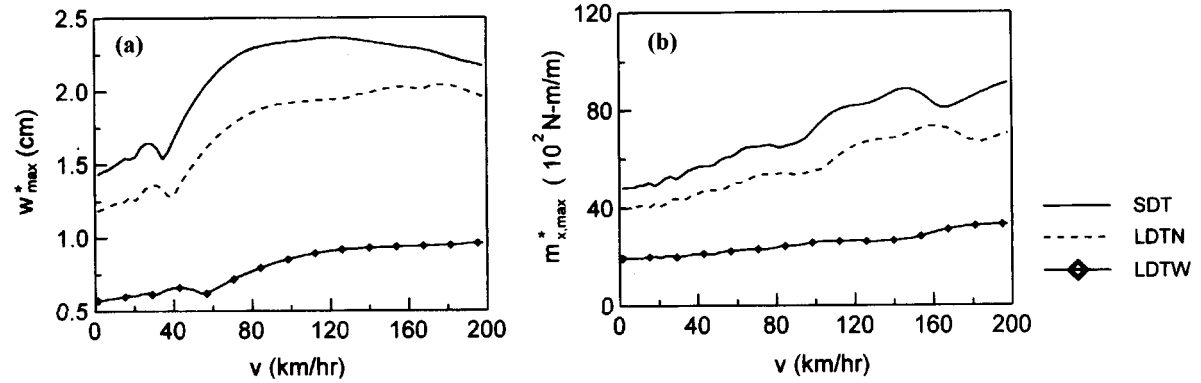

Fig. 6 Comparisons of the effects of three deflection theories on: (a) $w^*_{max}-v$ and (b) $m^*_{x,max}-v$ distributions of the Mindlin plate (a=b=20 m, h=0.1 m) due to a moving concentrated force ($4P_1$= 20 kN)

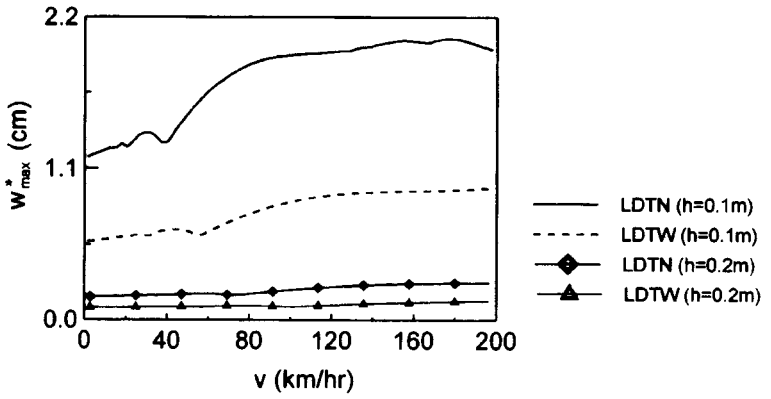

Fig. 7 Comparison of the effects of two values of thickness on the $w^*_{max} - v$ distribution of the Mindlin plate (a=b=20 m) due to a moving concentrated force ($4P_1$=20 kN)

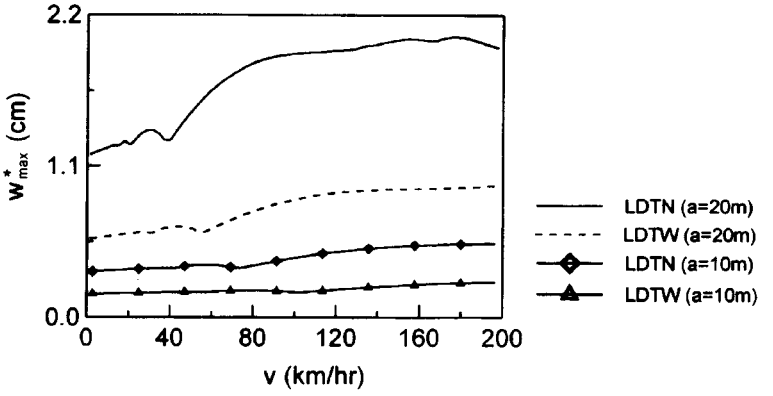

Fig. 8 Comparison of the effects of two values of area (a=b) on the $w^*_{max} - v$ distribution of the Mindlin plate (h=0.1 m) due to a moving concentrated force ($4P_1$=20 kN)

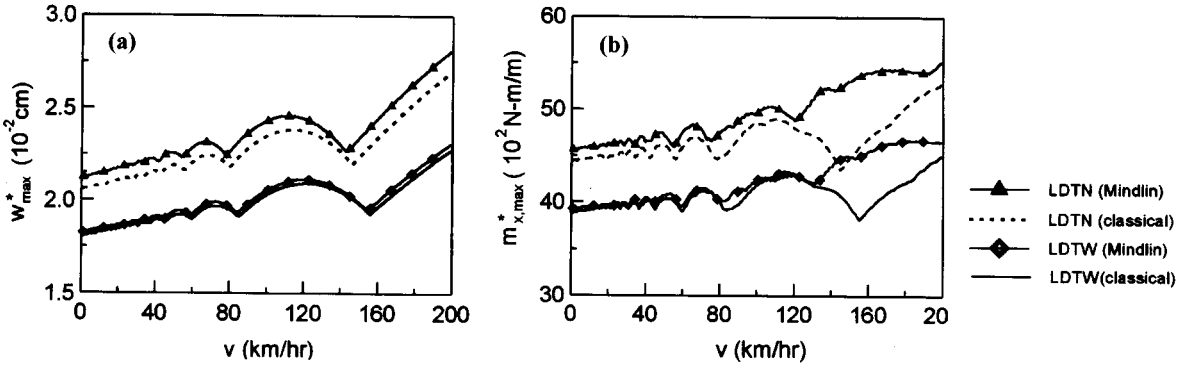

Fig. 9 Comparisons of the effects of two plate models on: (a) $w^*_{max} - v$ and (b) $m^*_{x,max} - v$ distributions of the plate (a=b=20 m, h=0.4 m) due to a moving concentrated force ($4P_1$=20 kN)

plate models on the $w^*_{max} - v$ distribution and the $m^*_{x,max} - v$ distribution of a square plate (a=b=20 m, h=0.1 m) induced by a moving concentrated force are displayed in Figs. 9(a) and 9(b), respectively. Results of both figures show that the effects of shear deformation and rotatory inertia of the plate cause both w^*_{max} and $m^*_{x,max}$ of the Mindlin plate to be greater than those of the classical plate.

9. Conclusions

The transverse deflection of a thin Mindlin plate caused by the weight of the plate is the same as that of the classical plate. The effect of in-plane extensions caused by the weight of the plate enlarges the modal frequencies of the plate. Furthermore, the product of dynamic deflection with the forces of the in-plane extensions, which is caused by the weight of the plate, stiffens the plate. A rapid moving force with a large magnitude causes the fundamental period of the plate to be small. The deviations of dynamic transverse deflection and of dynamic bending moment between the large deflection theory and the small deflection theory are significant for a thin plate with a large area. Both the dynamic transverse deflection and the dynamic moment of the Mindlin plate are greater than those of the classical plate.

References

Broyden, C.G. (1965), "A class of methods for solving nonlinear simultaneous equations", *Mathematics of Computation,* **19**, 577-593.

Celep, Z. (1980), "Shear and rotatory inertia effects on the large amplitude vibration of the initially imperfect plates", *Journal of Applied Mechanics,* **47**, 662-666.

Chu, H. and Herrmann, G. (1956), "Influence of large amplitude on free flexural vibrations of rectangular elastic plates", *Journal of Applied Mechanics,* **23**, 532-540.

Fung, Y.C. (1965), *Foundations of Solid Mechanics,* Prentice-Hall, Englewood Cliffs, NJ.

Mindlin, R.D. (1951), "Influence of rotatory inertia and shear on flexural motions of isotropic elastic plates", *Journal of Applied Mechanics,* **18**, 31-38.

Wang, R.T. and Lin, T.Y. (1996), "Vibration of multispan Mindlin plates to a moving load", *Journal of the Chinese Institute of Engineers,* **19**(4), 467-477.

Wu, C.S. and Vinson, J.R. (1969), "Influences of large amplitudes, transverse shear deformation, and rotatory inertia on lateral vibrations of transversely isotropic plates", *Journal of Applied Mechanics,* **36**, 254-260.

Appendix A

List of the ijth set of mode shape functions of the Mindlin plate

$$W^{(ij)}(\bar{x},\bar{y}) = \sin(i\pi\bar{x})\sin(j\pi\bar{y}) \tag{A1}$$

$$\Psi^{(ij)}_{\bar{x}}(\bar{x},\bar{y}) = B_{ij}\cos(i\pi\bar{x})\sin(j\pi\bar{y}) \tag{A2}$$

$$\Psi^{(ij)}_{\bar{y}}(\bar{x},\bar{y}) = C_{ij}\sin(i\pi\bar{x})\cos(j\pi\bar{y}) \tag{A3}$$

$$M^{(ij)}_{\bar{x}}(\bar{x},\bar{y}) = -\left(\frac{\partial\Psi^{(ij)}_{\bar{x}}}{\partial\bar{x}} + \mu\lambda^2\frac{\partial\Psi^{(ij)}_{\bar{y}}}{\partial\bar{y}}\right),\quad M^{(ij)}_{\bar{y}}(\bar{x},\bar{y}) = -\left(\frac{\mu}{\lambda^2}\frac{\partial\Psi^{(ij)}_{\bar{x}}}{\partial\bar{x}} + \frac{\partial\Psi^{(ij)}_{\bar{y}}}{\partial\bar{y}}\right),$$

$$M_{\bar{x}\bar{y}}^{(ij)}(\bar{x},\bar{y}) = -\frac{1-\mu}{2}\left(\frac{\partial \Psi_{\bar{x}}^{(ij)}}{\partial \bar{y}} + \frac{\partial \Psi_{\bar{y}}^{(ij)}}{\partial \bar{x}}\right), \quad Q_{\bar{x}}^{(ij)}(\bar{x},\bar{y}) = \frac{\partial W^{(ij)}}{\partial \bar{x}} - \Psi_{\bar{x}}^{(ij)},$$
$$Q_{\bar{y}}^{(ij)}(\bar{x},\bar{y}) = \frac{\partial W^{(ij)}}{\partial \bar{y}} - \Psi_{\bar{y}}^{(ij)} \tag{A4}$$

where

$$(B_{ij}, C_{ij}) = (i, j)\left\{\frac{(1-\mu)\pi^3\eta}{2}(i^2+\lambda^2 j^2) + \pi\eta\left(\eta - \frac{r^2\omega_{ij}^2}{12}\right)\right\} /$$
$$\left\{\frac{(1-\mu)\pi^4}{2}(i^2+\lambda^2 j^2)^2 + \left(\eta - \frac{r^2\omega_{ij}^2}{12}\right)\left(\frac{3-\mu}{2}\right)\pi^2(i^2+\lambda^2 j^2) + \left(\eta - \frac{r^2\omega_{ij}^2}{12}\right)^2\right\}$$